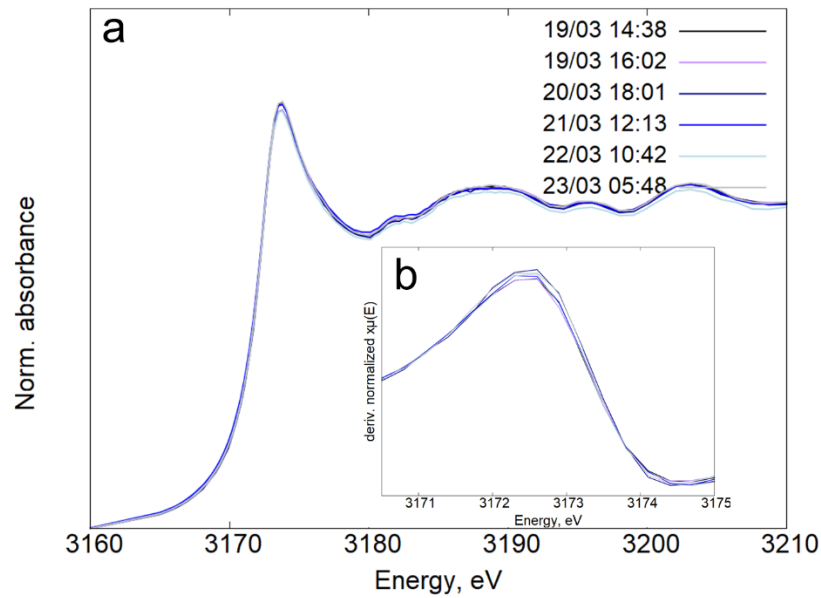


Supplementary material

**X-ray absorption records of Pd<sup>2+</sup> on Ni site in pentlandite**

Valeriya Brovchenko\*, Margarita Merkulova, Jonathan Sittner, Vladimir Shilovskih, Camelia Borca, Thomas Huthwelker, Sergey F. Sluzhenikin, Veerle Cnudde



**Figure S1.** (a) All Pd L<sub>3</sub>-edge XANES spectra of Pd foil measured during the beamtime; (b) First derivatives of Pd L<sub>3</sub>-edge XANES spectra of Pd foil.

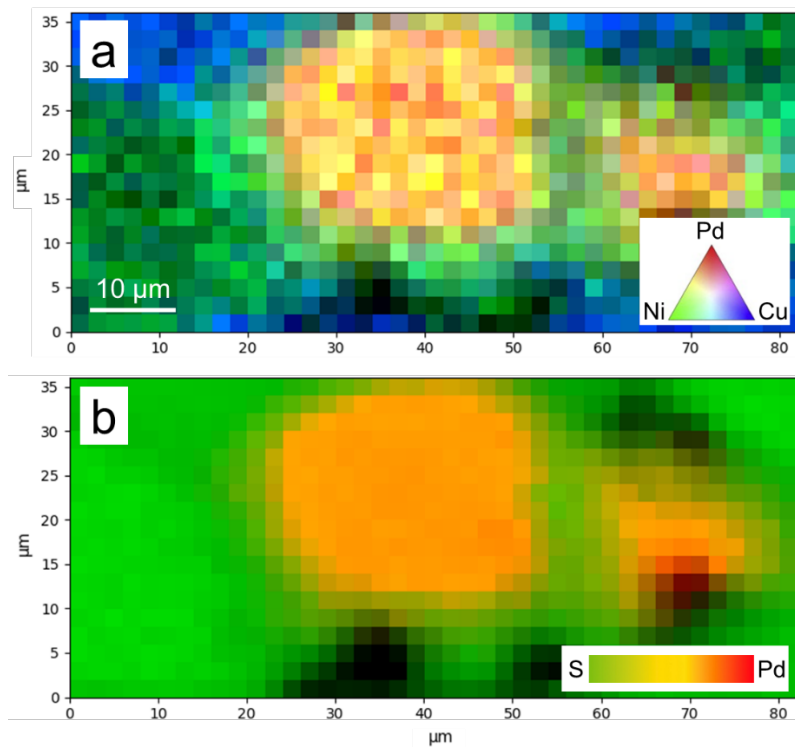


**Figure S2.** Micro-XRF map of a Pd-rich area in sample RM 29\_1\_1a. Pixel size 2×2 μm<sup>2</sup>.

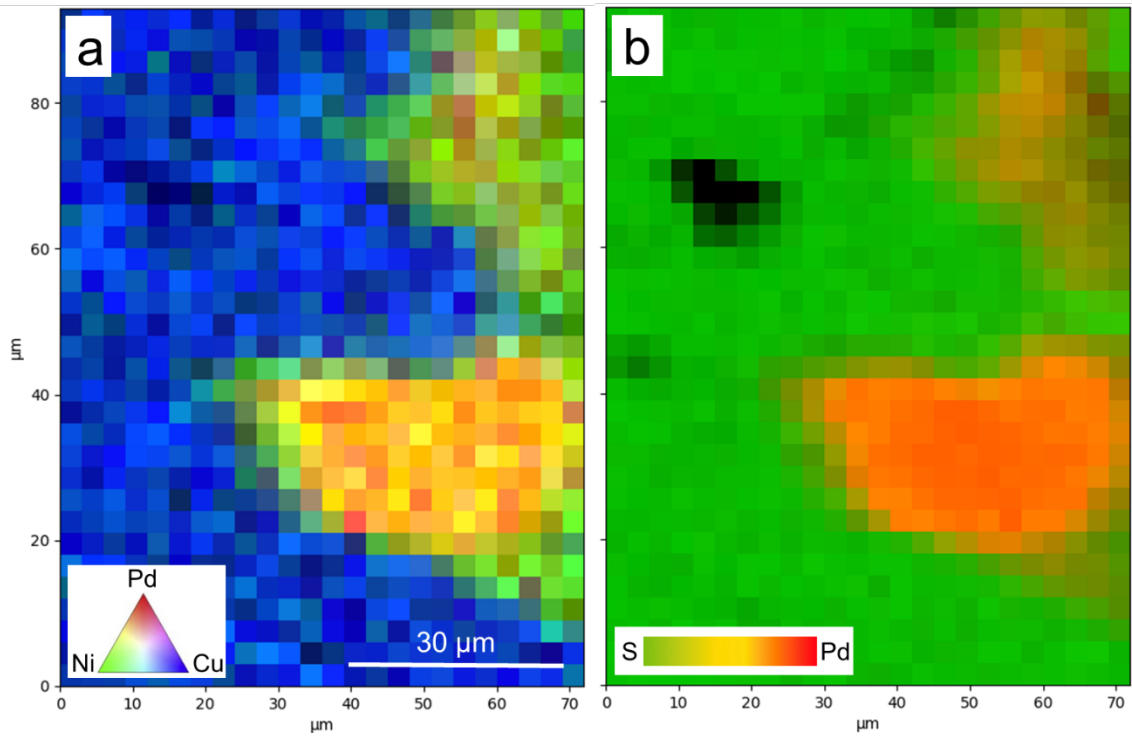


**Figure S3.** Micro-XRF map of a Pd-rich area in sample RM 29\_1\_8a. Pixel size  $3 \times 3 \mu\text{m}^2$ .

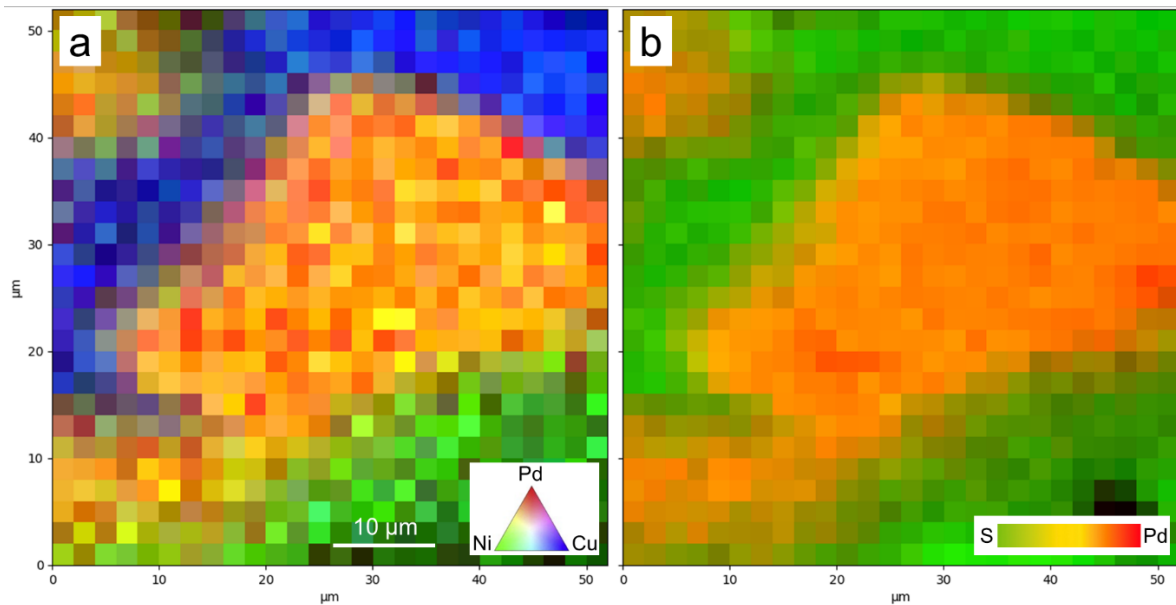


**Figure S4.** Micro-XRF map of a Pd-rich area in sample RM 29\_3\_7a. Pixel size  $2 \times 2 \mu\text{m}^2$ .

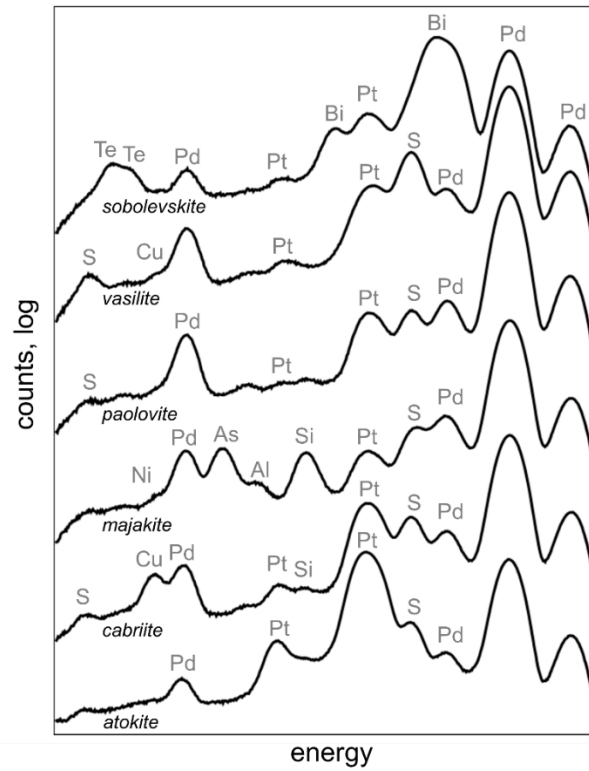


**Figure S5.** Micro-XRF spectra of six PGM grains from the Mineralogical Collections of the Technische Universität Bergakademie Freiberg (Germany). Spectra were recorded with 3174 eV incident beam and 300 s collection time.

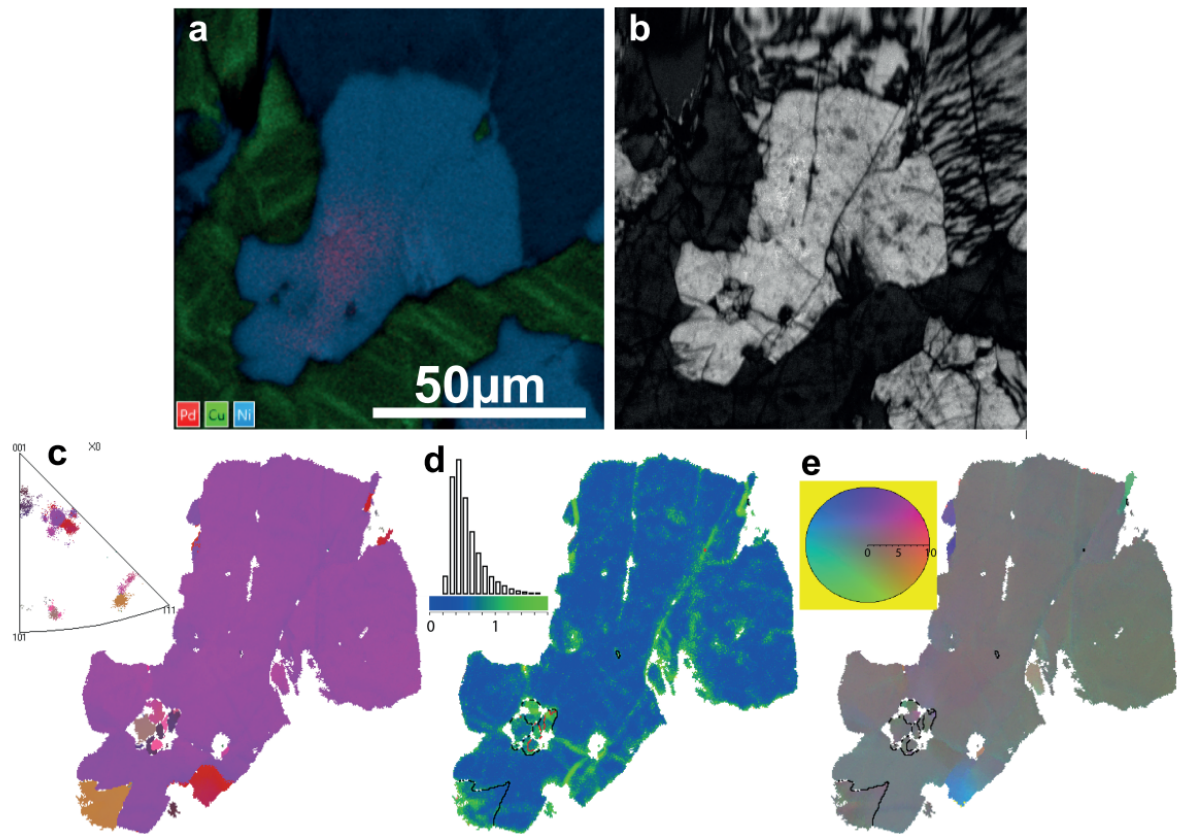


**Figure S6.** EBSD data collected from heterogeneous Pd-containing pentlandite grain in sample RM 30\_4, (a) EDX mapping of an area containing anomalous pentlandite grain in Ni, Cu and Pd characteristic x-rays; (b) diffraction quality map; (c) Euler-colored orientation map and corresponding inverse pole figure, (d) local misorientation map depicting local strains, deformations and local disorientation graph with no signs of local strains; (e) map of disorientation from average depicting grain modularity and disorientation directions and corresponding coloring legend.

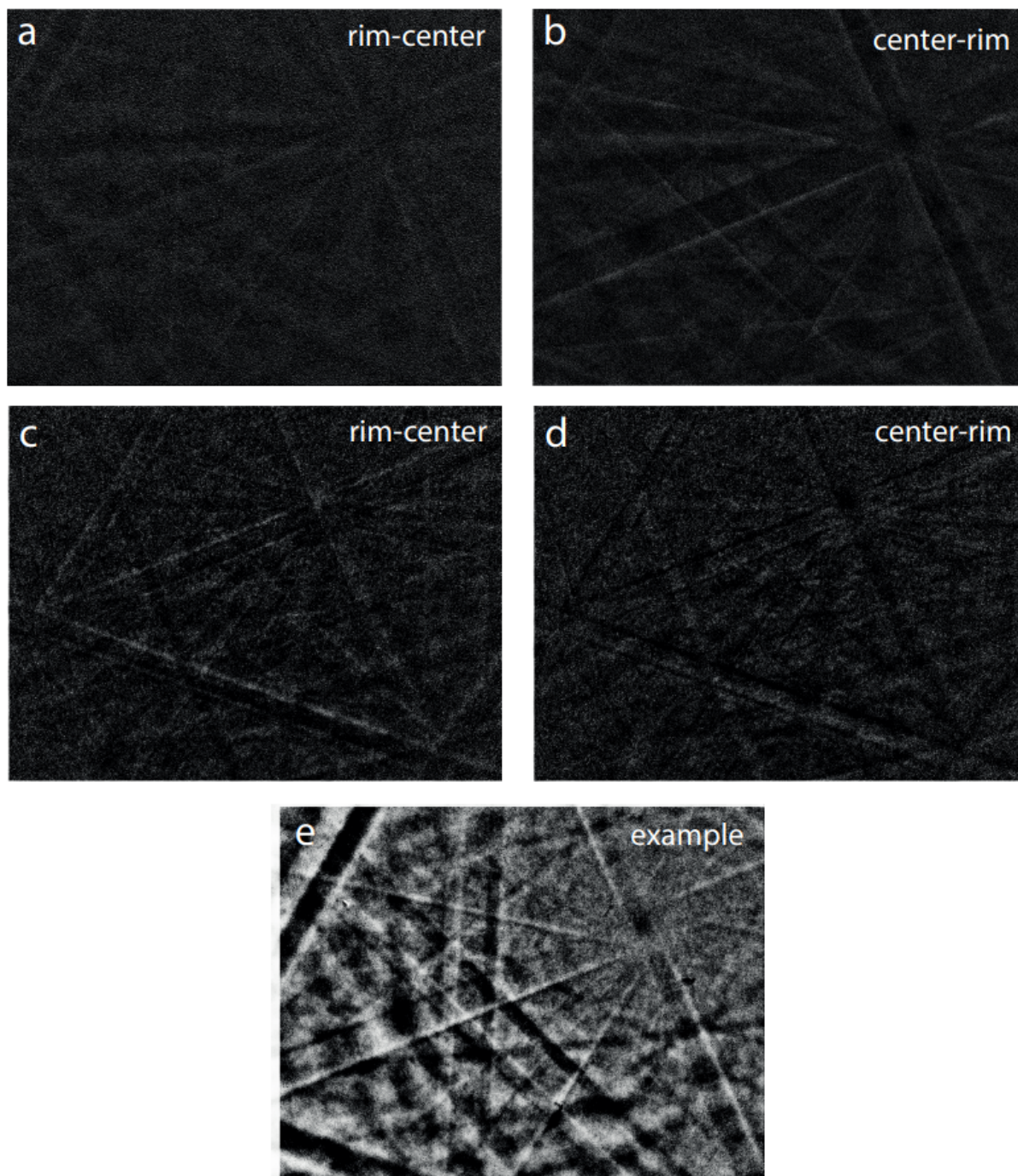


**Figure S7.** Differential EBSD patterns of Pd-containing pentlandite grains in sample RM 30\_4 depicting the subtraction of diffraction data of Pd rich centers from Pd-free rims (rim-center; **a,c**) and vice versa (center-rim; **b,d**). The **e** image corresponds to a noncorcondant image and is an example.

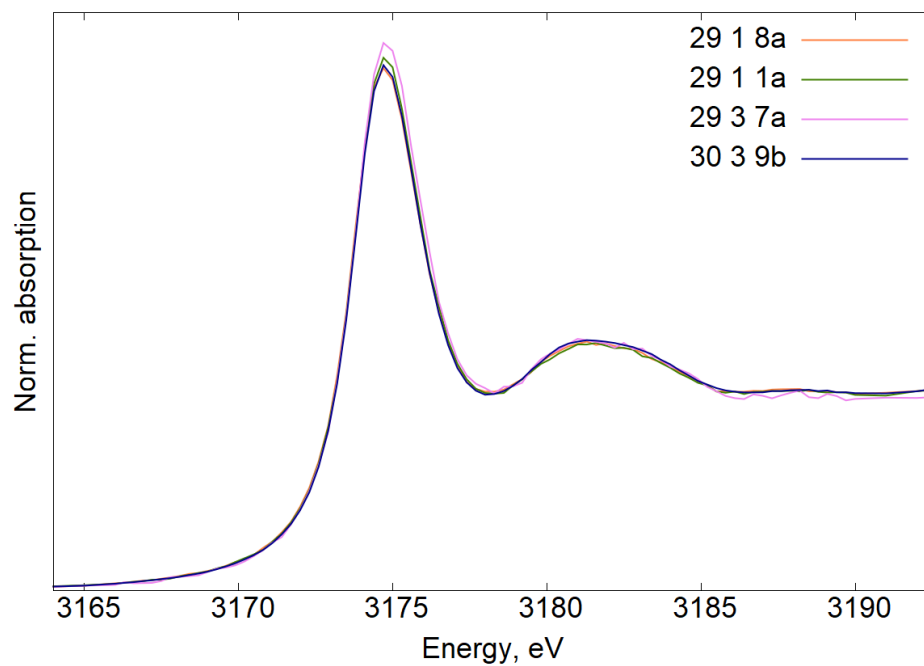


**Figure S8.** Pd L<sub>3</sub>-edge XANES spectra of four pentlandite grains from samples RM 29\_1\_8a, Rm 29\_1\_1a, RM 29\_3\_7a, and RM 30\_3\_9b.

**Table S1.** Composition of pentlandite from Mt. Rudnaya (Norilsk, Russia) by EPMA. Values are in wt.%. D.L. – detection limit; b.d.l. – below detection limit.

	<i>d.l.</i>	<i>0.08</i>		<i>0.07</i>		<i>0.06</i>		<i>0.02</i>	<i>0.04</i>	
<b>No.</b>	<b>Sample</b>	<b>Cu</b>	<b>S</b>	<b>Pt</b>	<b>Ni</b>	<b>Co</b>	<b>Fe</b>	<b>Pd</b>	<b>Ag</b>	<b>Total</b>
1	RM30	0.34	33.00	b.d.l.	36.59	0.30	27.32	1.14	b.d.l.	98.68
2	RM30	0.20	32.72	0.08	36.25	0.30	27.92	2.14	b.d.l.	99.60
3	RM29	0.10	33.48	b.d.l.	38.08	0.42	27.68	b.d.l.	0.07	99.76
4	RM29	0.19	33.41	b.d.l.	38.65	0.44	27.71	0.02	b.d.l.	100.42
5	RM29	0.20	33.37	b.d.l.	38.00	0.38	28.05	0.30	b.d.l.	100.31
6	RM29	0.20	32.86	0.07	35.72	0.42	27.83	2.91	b.d.l.	100.01
7	RM29	0.20	32.60	b.d.l.	34.17	0.33	27.53	4.84	b.d.l.	99.67
8	RM29	0.28	33.12	b.d.l.	35.67	0.33	28.05	3.29	b.d.l.	100.73
9	RM29	0.32	33.17	b.d.l.	36.61	0.38	28.42	1.59	b.d.l.	100.48
10	RM29	0.20	33.11	b.d.l.	37.31	0.43	27.83	0.90	b.d.l.	99.77
11	RM29	0.22	33.09	b.d.l.	36.13	0.41	28.07	2.22	0.08	100.13
12	RM29	0.26	32.89	0.09	35.42	0.38	27.82	3.61	0.06	100.45
13	RM29	0.20	32.99	b.d.l.	35.80	0.34	28.02	2.70	0.06	100.05
14	RM29	0.21	32.95	b.d.l.	36.74	0.38	28.09	1.79	b.d.l.	100.15
15	RM29	0.29	33.44	0.08	37.00	0.37	28.17	1.27	b.d.l.	100.61
16	RM29	0.27	33.01	0.10	37.52	0.40	28.14	0.77	b.d.l.	100.21
17	RM29	0.28	32.49	0.1	34.62	0.37	27.73	4.62	b.d.l.	100.2
18	RM29	0.16	32.79	b.d.l.	38.07	0.38	27.34	0.07	b.d.l.	98.81
19	RM29	0.12	32.97	b.d.l.	37.99	0.45	27.42	0.28	b.d.l.	99.22